Available online at www.sciencedirect.com
ScienceDirect
Trans. Nonferrous Met. Soc. China 29(2019) 785−790
Transactions of Nonferrous Metals Society of China
www.tnmsc.cn

Preparation and electro-catalytic activity of nanoporous palladium by dealloying rapidly-quenched $Al_{70}Pd_{17}Fe_{13}$ quasicrystalline alloy

Xin-yi LIU, Ying-min WANG, Jian-bing QIANG, Bao-lin WANG, Dian-guo MA, Wei ZHANG, Chuang DONG

Key Laboratory of Materials Modification by Laser, Ion, and Electron Beams (Dalian University of Technology), Ministry of Education, Dalian 116024, China

Received 24 April 2018; accepted 13 August 2018

Abstract: The formation of nanoporous Pd was studied by electro-chemical dealloying a rapidly-quenched $Al_{70}Pd_{17}Fe_{13}$ quasicrystal alloy in dilute NaCl aqueous solution, and the electro-catalytic activity of the nanoporous Pd towards methanol electro-oxidation was evaluated by cyclic voltammetry in 1 mol/L KOH solution. XRD and TEM analyses revealed that nano-decomposition of quasicrystal grains occurred in the initial stage of dealloying, and the fully dealloyed sample was composed of FCC-Pd phase. Scanning electron microscopy observation indicated that a maze-like nanoporous pattern was formed in the dealloyed sample, consisting of percolated pores of 5−20 nm in diameter in a skeleton of randomly-orientated Pd nano-ligaments with a uniform thickness of ~5 nm. A retention of ~12 at.% Al in the Pd nano-ligments was determined by energy dispersive X-ray spectroscopy (EDS). The nanoporous Pd demonstrated obvious electro-catalytic activity towards methanol electro-oxidation in alkaline environment.

Key words: nanoporous palladium; Al−Pd−Fe quasicrystal; dealloying; electro-catalytic activity

1 Introduction

Dealloying is a corrosion process during which one or several component elements are selectively dissolved out from an alloy [1,2]. This corrosion process has long been known to play a crucial role in stress-corrosion-cracking of industrial alloys [3,4]. Recently, there has been a revived interest in dealloying because such a corrosion process can generate useful bulk nanoporous metals [5]. Nanoporous metals made by dealloying can take the form of millimeter-sized bodies with a bicontinuous microstructure comprised of nanoscale pores and metal ligaments. The size of metal ligament can reach down to the very limits of stability of nanoscale solids. These bulk nanomaterials combine properties characteristic of metals, such as good electrical conductivity and catalytic activity, with the extreme properties of nanostructures including the large surface-to-volume ratio, which give rise to their potential applications in the area of catalysis, sensing and nanomechanics [5−7].

Metallic alloys of different types of structures have been used as the starting materials for the fabrication of nanoporous metals by dealloying. Most of the nanoporous metals are made from single-phase solid solution alloys [8−13]. Some amorphous alloys are found to be suitable dealloying precursors. Nanoporous Pd, Au (Pd), Cu, Ni and Pt metals have been fabricated by means of electrochemical dealloying the melt-spun metallic glasses of $Pd_{30}Ni_{50}P_{20}$ [14], $Au_{30}Si_{20}Cu_{33}$-Ag_7Pd_{10} [15], $Al_{70}Cu_{18}Mg_{12}$ and $Al_{73}Cu_{16}Mg_8Ni_3$ [16], $Zr_{67}Ni_{33}$ [17], $Fe_{60}Pt_{10}B_{30}$ [18], as well as the electron beam deposited $Pt_{100-x}Si_x$ amorphous films [19]. The study of dealloying has also been extended into several two-phase alloy systems [20−23]. In these two-phase alloys, dealloying has been found to occur in some intermetallic phases. For instance, in a rapidly-quenched $Al_{70}Pd_{30}$ alloy composed of Al_3Pd and Al_3Pd_2 phases, Al_3Pd turns into nanoporous Pd after dealloying, and Al_3Pd_2 remains intact in the dealloyed structure [23]. Regardless of their structure differences, the above mentioned precursor alloys share a common electrochemical characteristic: to make dealloying occur, it is necessary that the difference between the single electrode potentials of the constituent metals in the

Foundation item: Project (51671045) supported by the National Natural Science Foundation of China; Project (DUT18GF112) supported by the Fundamental Research Funds for the Central Universities, China; Project (TZ2016004) supported by the Science Challenge Project, China

Corresponding author: Ying-min WANG; Tel: +86-411-84709336; E-mail: apwangym@dlut.edu.cn

DOI: 10.1016/S1003-6326(19)64988-5

electrolyte is sufficiently large, and that the potential of the dissolving alloy is higher than that of the less noble metal [24].

The component elements of Al-based Al−Pd−TM (TM: transition metals) icosahedral quasicrystals (*i*-phases) [25,26] also exhibit such an electrochemical characteristic. In the Al−Pd−Fe system, a nearly single-phase icosahedral quasicrystalline alloy can be made by melt-quenching at the composition of $Al_{70}Pd_{17}Fe_{13}$ [27]. The standard electrode potentials of Al (−1.662 V (vs SHE)) and Fe (−1.185 V (vs SHE)) are strongly more negative than that of Pd (0.951 V (vs SHE)). Moreover, the dealloyable Al_3Pd phase happens to be a crystalline approximant of the *i*-phase, which has the same local structures as the quasicrystal but is lack of quasi-periodic order [25,27]. It is therefore expected that selective dissolution of the less noble Al and Fe atoms from *i*-$Al_{70}Pd_{17}Fe_{13}$ may be realized under favorable electrochemical conditions. The previous studies on the surface corrosion property of Al−Cu−Fe (or Co) icosahedral and decagonal phases showed that unique nano-cuboid Cu could be made by chemical leaching the samples in concentrated NaOH aqueous solutions [28−31]. So, it is also tempting to think that a unique nanoporous pattern may be obtained from *i*-$Al_{70}Pd_{17}Fe_{13}$, as the structure order of an icosahedral phase is fundamentally different from those of crystalline and amorphous alloys. In this work, the fabrication of nanoporous Pd was investigated by dealloying a rapidly-quenched *i*-$Al_{70}Pd_{17}Fe_{13}$ alloy in dilute NaCl aqueous solution. Structure evolution of *i*-$Al_{70}Pd_{17}Fe_{13}$ upon electrochemical polarization was characterized for both the partially and fully dealloyed samples, and a primary study of the electro-catalytic activity of the nanoporous Pd metal towards methanol oxidation in alkaline environment was also carried out.

2 Experimental

Alloy buttons with a nominal composition of $Al_{70}Pd_{17}Fe_{13}$ (at.%) were prepared by arc melting appropriate amounts of Al (99.99 wt.%), Pd (99.99 wt.%) and Fe (99.50 wt.%) in a Ti-gettered Ar atmosphere under a background vacuum level of 5×10^{-3} Pa. Using the alloy buttons, ribbon samples with cross-sectional dimensions of ~0.02 mm × 2 mm were made using a single roller melt-spinner. The as-quenched and dealloyed samples were ground into powders for phase identification by X-ray diffraction (Cu K_α, λ=0.15406 nm) operated at a tube voltage of 40 kV. The morphology and composition of samples before and after dealloying were studied using a Hitachi S−4800 scanning electron microscope (SEM) equipped with an Oxford energy dispersive X-ray spectroscope (EDS), operated at an accelerating voltage of 15 kV. The microstructure observation was carried out with a Tecnai G220 S-Twin transmission electron microscope (TEM) operated at 200 kV. A standard three-electrode cell, in which a Ag/AgCl electrode in saturated KCl was adopted as the reference electrode, and pure platinum and the *i*-$Al_{70}Pd_{17}Fe_{13}$ ribbon alloy as the counter and working electrodes, respectively, were used to perform electrochemical dealloying, driven by an external potential of 0.05 V (vs Ag/AgCl) in 0.1 mol/L NaCl aqueous solution. The electrochemical properties of freshly prepared nanoporous Pd were measured in 1 mol/L KOH and a mixed solution of 1 mol/L KOH + 0.5 mol/L CH_3OH at a sweeping rate of 20 mV/s, respectively. The electrochemical experiments were carried out at room temperature. The samples subjected to dealloying for 5 and 40 min were determined as the partially and fully dealloyed states, respectively, to examine the structure evolution of *i*-$Al_{70}Pd_{17}Fe_{13}$ during dealloying.

3 Results and discussion

3.1 Structure evolution of *i*-$Al_{70}Pd_{17}Fe_{13}$ upon dealloying

Figure 1(a) presents the XRD patterns of the as-quenched, partially and fully dealloyed $Al_{70}Pd_{17}Fe_{13}$ samples. The as-quenched alloy is composed of the *i*-phase as the majority phase and a minor amount of Al_3Pd. Comparing the powder diffraction patterns of the as-quenched and partially dealloyed samples, it is found that the intensity ratio of (202)-Al_3Pd and (20/32)-*i* peaks increases after a certain time of dealloying. This result indicates that the volume fraction of *i*-phase is reduced in the partially dealloyed sample. Apart from this, a diffused diffraction hump appears at $2\theta\approx40°$ in the diffraction pattern. The partially dealloyed micro-structure was further studied by TEM. A typical high resolution TEM image of partially dealloyed *i*-phase grains is shown in Fig. 1(b). It is seen that a small portion of the *i*-phase grain has been dealloyed into a collection of randomly orientated nano-ligaments. The polycrystalline array of interconnected nano-ligaments is distinctly different from the lattice-coherency nature of the nano-ligaments derived from crystalline solid solution alloys [32,33]. The remaining part of the grain decomposes into a mixture of nanocrystals, which is corroborated by the selected area electron pattern of the Debye−Sherrer ring form. Some *i*-phase nanoparticles still survive in the decomposed grain, coexisting with the randomly-orientated nanocrystals. The microstructural evidence indicates that nano-decomposition of *i*-phase grains occurs firstly in the initial stage of dealloying. In the fully dealloyed sample, both *i*-phase and Al_3Pd

phases disappear, and a single FCC phase is formed. The broadened diffraction peaks are indicative of an ultrafine grain size of the FCC phase (Fig. 1(a)).

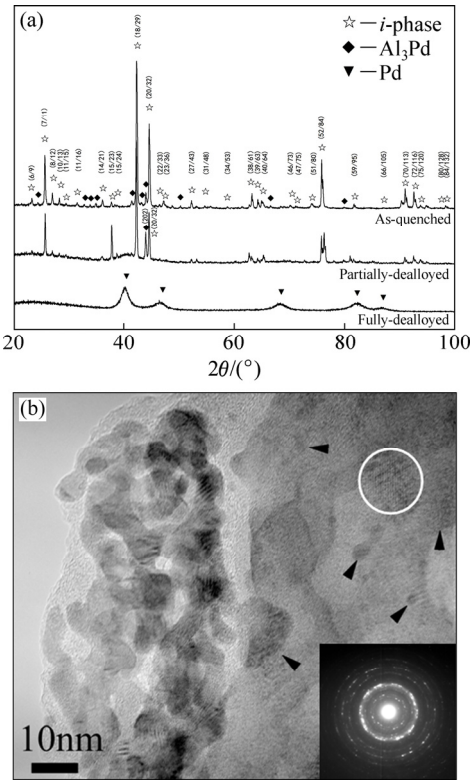

Fig. 1 XRD patterns showing structure evolution of rapidly-quenched $Al_{70}Pd_{17}Fe_{13}$ alloy during dealloying process (Cahn's main indices are used to index the *i*-phase) (a) and high resolution TEM image showing nano-decomposition of *i*-phase grain (The black arrows point to randomly nucleated nanocrystals. The circled zone is a surviving *i*-phase nanoparticle. The inset at the bottom-right corner is the selected area electron diffraction pattern taken from the remaining portion of the *i*-phase grain which is nano-decomposed) (b)

3.2 Nanoporous structure of dealloyed *i*-$Al_{70}Pd_{17}Fe_{13}$

The surface morphology of the as-quenched *i*-$Al_{70}Pd_{17}Fe_{13}$ is shown by the SEM image in Fig. 2(a). The grain size is not uniform, living in a range from several hundred nanometers to a few micrometers. The grain surface exhibits a fractal-like morphology, which is typical for icosahedral quasicrystals. A number of voids are formed at grain boundaries, which, upon dealloying, can provide paths for rapid passage of electrolyte into the interior of the sample. While the *i*-phase sample was dealloyed in NaCl aqueous solution, gas bubbles evolved vigorously and continuously from the sample surface. Since the potential of gas evolution is well below the Cl_2 and O_2 evolution potentials, it is inferred that this process is corresponding to H_2 evolution due to the reaction of the alloy surface atoms with the solution. Intergranular cracks are observed in the dealloyed samples (Fig. 2(b)). The shapes of *i*-phase grain are preserved, and a maze-like nanoporous pattern is formed on the grain surface (Fig. 2(c)). The pore size in the nanoporous surface is ~10 nm. The cross-sectional fracture surface of a fully dealloyed sample is shown in Fig. 2(d). The interior structure of the bulk sample is comprised of interconnected nano-ligaments of ~5 nm in thickness and pores of 5−20 nm in diameter. This kind of nanoporous pattern has formed throughout the entire sample interior, suggesting that the Al_3Pd phase has also been dealloyed. The EDS analysis revealed the retentions of ~12 at.% Al and a negligible amount of Fe in the Pd nano-ligaments.

Though the electrochemical process occurring at the quasicrystal/electrolyte interface is hard to be clarified, the surface atomic structure of *i*-$Al_{70}Pd_{17}Fe_{13}$ is believed to play a crucial role for the initiation of dealloying. In the *i*-phase structure, two types of pseudo-Mackay icosahedra consisting of successive atomic shells are the basic structural units, in which Al atoms form the external shells [34,35]. These pseudo-Mackay clusters are hierarchically organized into large building blocks and grow into infinity in the quasiperiodic lattice. It is also known that the surface atomic structure of *i*-phase is bulk-terminated, i.e. the surface layer planes are identical to planes from the bulk model of the quasicrystal [36,37]. In view of the surface atomic structure characteristic, a structural evolution mechanism involved in the dealloying process is proposed for *i*-$Al_{70}Pd_{17}Fe_{13}$. In the NaCl aqueous solution and under an appropriate external potential, electrochemical attack on the quasicrystal surface is readily initiated locally at the shell surface Al atom sites of pseudo-Mackay clusters. After a certain amount of Al atoms have been removed from the cluster surface shells and dissolved into the electrolyte, the long-range connection of pseudo-Mackay icosahedra is broken in the *i*-phase structure. This leads to nano-decomposition of *i*-phase grains. With continuous dissolution of Al and Fe atoms, the *i*-phase nanoparticles are further dealloyed. The remaining Pd atoms are driven to agglomerate into clusters, and interconnected Pd nano-ligaments eventually form via a self-assembly process. This structural evolution process entails exposing fresh quasicrystal surfaces to the electrolyte, which sustains the propagation of dealloying.

3.3 Catalytic activity of NP-Pd(Al) towards methanol electro-oxidation

The electrochemical properties of the nanoporous Pd for methanol electro-oxidation were primarily evaluated by cyclic voltammetry (CV) in KOH solutions with and without methanol. For comparison, the voltammetric behaviors of a bulk Pd metal were also measured under otherwise identical conditions. Figure 3 compares the CV curves of the nanoporous Pd in 1 mol/L

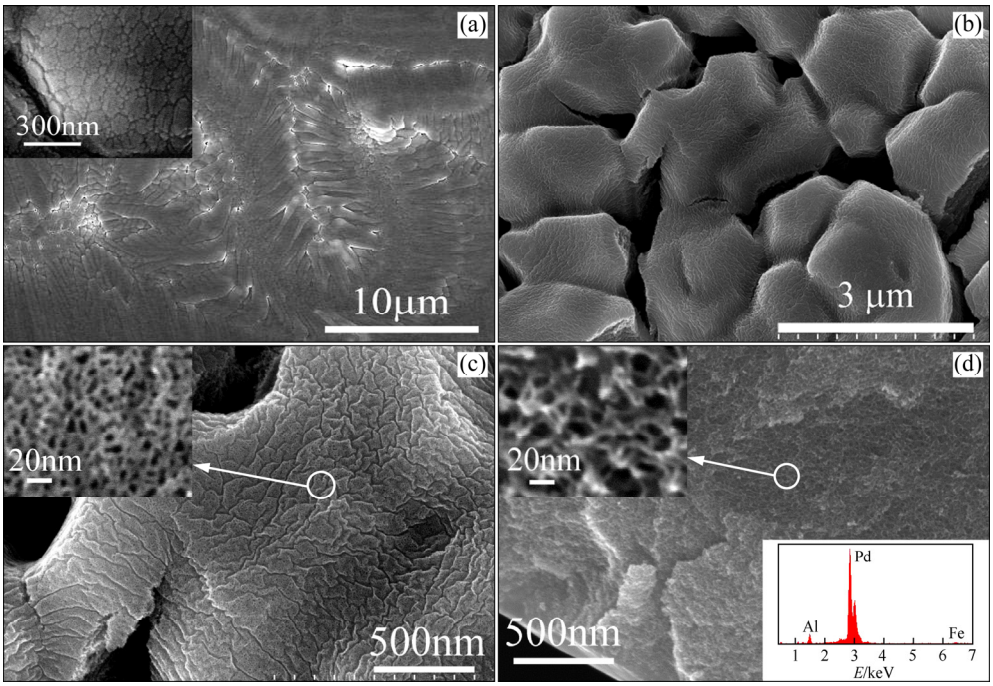

Fig. 2 SEM image showing surface morphology of rapidly-quenched $Al_{70}Pd_{17}Fe_{13}$ (The inset shows the fractal-like surface of *i*-phase grains) (a), overview of surface morphology of fully-dealloyed sample (b), nanoporous pattern formed on the grain surface (The inset is a high magnification image showing the length scales of pores and ligaments) (c) and SEM image taken from cross-sectional fracture surface of dealloyed sample (The inset at the top-left corner showing the nanoporous pattern formed in the interior region of the sample, the bottom-right corner inset being the EDX spectrum taken from the nano-ligaments) (d)

KOH with and without 0.5 mol/L CH_3OH. The forward scan CV curve of the nanoporous Pd in 1 mol/L KOH exhibits a weak oxidation peak around −0.45 V, which is attributed to the formation of Pd oxide layer on the nanoporous electrode surface [38]. A strong and broad oxidation peak appears in the potential range from −0.69 to 0.2 V in the forward scan CV curves of the nanoporous Pd electrode in the mixed solution, which corresponds to oxidation of chemisorbed species coming from methanol absorption [39,40]. The onset potential of methanol oxidation on the nanoporous Pd surface decreases by 0.17 V compared with that for bulk Pd, indicating that the electro-oxidation kinetics is greatly enhanced on the nanoporous surface. A maximal apparent current density of 117 mA/cm^2 is read from the oxidation peak of the nanoporous Pd, and that for bulk Pd is about 1 mA/cm^2. The characteristic of forward scan CV curve reveals evident electro-catalytic activity of the nanoporous Pd in the alkaline environment. Comparison of the series of CV curves indicates that the maximal apparent current density gets slightly decreased with increasing cycle times. The electro-catalytic performance is mainly ascribed to the large surface area of the nanoporous Pd, which offers a huge number of surface defects as active sites for the absorption and oxidation of methanol molecules. A thorough understanding of electro- oxidation process occurring on the nanoporous Pd surface requires knowledge of the surface adsorption of various species, the alloying effect of Al on the electronic structure of Pd, and so forth. Further experimental evidence is needed for a comprehensive study of this phenomenon.

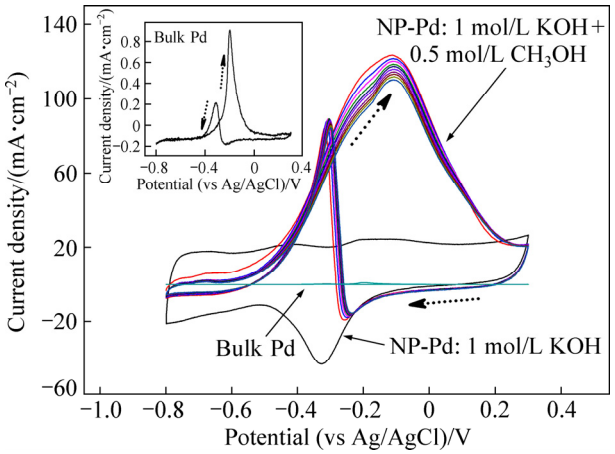

Fig. 3 CV curves of nanoporous Pd in 1 mol/L KOH and mixed 1 mol/L KOH + 0.5 mol/L CH_3OH solutions (The inset is the CV curve of bulk Pd metal measured under identical electrochemical conditions. An apparent current density, which is worked out with the surface area of the bulk samples, is used in this plot. The directions of the forward and backward potential scans are designated by dash-dotted arrows. Sweeping rate: 20 mV/s, NP: Nanoporous)

4 Conclusions

(1) The electrochemical dealloying of a rapidly-quenched $Al_{70}Pd_{17}Fe_{13}$ quasicrystal alloy in dilute NaCl aqueous solution, and the catalytic activity of the dealloying product towards electro-oxidation of methanol in alkaline environment were investigated.

(2) The rapidly-quenched alloy was composed of *i*-$Al_{70}Pd_{17}Fe_{13}$ as the majority phase and a minor amount of Al_3Pd phase. Nano-decomposition of quasicrystal grains occurred in the initial stage of dealloying. After dealloying, the *i*-$Al_{70}Pd_{17}Fe_{13}$ and Al_3Pd phases transformed into FCC-Pd.

(3) The fully-dealloyed sample exhibited a nanoporous structure, consisting of a system of nanoscale pores in a skeleton of randomly orientated Pd nanoligaments of uniform thickness. A retention of ~12 at.% Al was found in the nano-ligaments.

(4) This nanoporous Pd metal exhibited evident catalytic activity towards electro-oxidation of methanol in alkaline environment.

References

[1] NEWMAN R C, SIERADZKI K. Metallic corrosion [J]. Science, 1994, 263: 1708−1710.

[2] ERLEBACHER J, SIERADZKI K. Pattern formation during dealloying [J]. Scripta Materialia, 2003, 49: 991−996.

[3] LI Rong, SIERADZKI K. Ductile-brittle transition in random porous Au [J]. Physical Review Letters, 1992, 68: 1168−1171.

[4] MARCUS P. Stress corrosion cracking mechanisms in theory and practice [M]. 2nd ed. New York: Marcel Dekker, 2002: 399−450.

[5] ERLEBACHER J, SESHADRI R. Hard materials with tunable porosity [J]. Materials Research Society Bulletin, 2009, 34: 561−568.

[6] WEISSMÜLLER J, NEWMAN R C, JIN H J, HODGE A M, KYSAR J W. Nanoporous metals by alloy corrosion: Formation and mechanical properties [J]. Materials Research Society Bulletin, 2009, 34: 577−586.

[7] DING Yi, CHEN Ming-wei. Nanoporous metals for catalytic and optical applications [J]. Materials Research Society Bulletin, 2009, 34: 569−576.

[8] PUGH D V, DURSUN A, CORCORAN S G. Formation of nanoporous platinum by selective dissolution of Cu from $Cu_{0.75}Pt_{0.25}$ [J]. Materials Research Society Bulletin, 2003, 18: 216−221.

[9] DING Yi, KIM Young-ju, ERLEBACHER J. Nanoporous gold leaf: Ancient technology/advanced materials [J]. Advanced Materials, 2004, 21: 1897−1900.

[10] SUN Li, CHIEN Chia-ling, SEARSON P C. Fabrication of nanoporous nickel by electrochemical dealloying [J]. Chemistry of Materials, 2004, 16: 3125−3129.

[11] HAYES J R, HODGE A M, BIENER J, HAMZA A V, SIERADZKI K. Monolithic nanoporous copper by dealloying Mn−Cu [J]. Journal of Materials Research, 2006, 21: 2611−2616.

[12] HAKAMADA M, MABUCHI M. Fabrication of nanoporous palladium by dealloying and its thermal coarsening [J]. Journal of Alloys and Compounds, 2009, 479: 326−329.

[13] ZHANG Xing-ming, LI Yan-xiang, ZHANG Hua-wei, LIU Yuan. Evolution of porous structure with dealloying corrosion on Gasar Cu−Mn alloy [J]. Transactions of Nonferrous Metals Society of China, 2015, 25: 1200−1205.

[14] YU Jing-shan, DING Yi, XU Cai-xia, INOUE A, SAKURAI T, CHEN Ming-wei. Nanoporous metals by dealloying multicomponent metallic glasses [J]. Chemistry of Materials, 2008, 20: 4548−4550.

[15] LANG X Y, GUO H, CHEN L Y, KUDO A, YU J S, ZHANG W, INOUE A, CHEN M W. Novel nanoporous Au−Pd alloy with high catalytic activity and excellent electrochemical stability [J]. Journal of Physical Chemistry C, 2010, 114: 2600−2603.

[16] ABURADA T, FITZ-GERALD J M, SCULLY J R. Synthesis of nanoporous copper by dealloying of Al−Cu−Mg amorphous alloys in acidic solution: The effect of nickel [J]. Corrosion Science, 2011, 53: 1627−1632.

[17] MIHAILOV L, REDZHEB M, SPASSOV T. Selective dissolution of amorphous and nanocrystalline Zr_2Ni [J]. Corrosion Science, 2013, 74: 308−313.

[18] OU Shu-li, MA Dian-guo, LI Yan-hui, YUBUTA K, TAN Zheng-quan, WANG Ying-min, ZHANG Wei. Fabrication and electrocatalytic properties of ferromagnetic nanoporous PtFe by dealloying an amorphous $Fe_{60}Pt_{10}B_{30}$ alloy [J]. Journal of Alloys and Compounds, 2017, 706: 215−219.

[19] THORP J C, SIERADZKI K, TANG Lei, CROZIER P A, MISRA A, NASTASI M, MITLIN D, PICRAUX S T. Formation of nanoporous noble metal thin films by electrochemical dealloying of Pt_xSi_{1-x} [J]. Applied Physics Letter, 2006, 88: 033110.

[20] ZHAO Chang-chun, WANG Xiao-guang, QI Zhen, JI Hong, ZHANG Zhong-hua. On the electrochemical dealloying of Mg−Cu alloys in a NaCl aqueous solution [J]. Corrosion Science, 2010, 52: 3962−3972.

[21] LU Hai-bo, LI Ying, WANG Fu-hui. Dealloying behavior of Cu−20Zr alloy in hydrochloric acid solution [J]. Corrosion Science, 2006, 48: 2106−2119.

[22] LU Hai-bo, LI Ying, WANG Fu-hui. Synthesis of porous copper from nanocrystalline two-phase Cu−Zr film by dealloying [J]. Scripta Materialia, 2007, 56: 165−168.

[23] WANG Xiao-guang, WANG Wei-min, QI Zhen, ZHAO Chang-chun, JI Hong, ZHANG Zhong-hua. Fabrication, microstructure and electrocatalytic property of novel nanoporous palladium composites [J]. Journal of Alloys and Compounds, 2010, 508: 463−470.

[24] ERLEBACHER J. An atomistic description of dealloying porosity evolution, the critical potential, and rate-limiting behavior [J]. Journal of the Electrochemical Society, 2004, 151: C614−C626.

[25] GOLDMAN A I, KELTON R F. Quasicrystals and crystalline approximants [J]. Reviews of Modern Physics, 1993, 65: 213−230.

[26] DONG Chuang, QIANG Jian-bing, WANG Ying-min, JIANG Nan, WU Jiang, THIEL P. Cluster-based composition rule for stable ternary quasicrystals in Al−(Cu, Pd, Ni)−TM systems [J]. Philosophical Magazine, 2006, 86: 263−274.

[27] TSAI A P, YOKOYAMA Y, INOUE A, MASUMOTO T. Quasicrystals in Al−Pd−TM (TM=transition metals) systems prepared by rapid solidification [J]. Japanese Journal of Applied Physics, 1990, 29: L1161−L1164.

[28] LOWE M, YADAV T P, FOURNÉE V, LEDIEU J, MCGRATH R, SHARMA H R. Influence of leaching on surface composition, microstructure, and valence band of single grain icosahedral Al−Cu−Fe quasicrystal [J]. Journal of Chemical Physics, 2015, 142: 094703.

[29] YADAV T P, MISHRA S S, SRIVASTAVA O N. Copper nanocubes on $Al_{65}Cu_{20}Fe_{15}$ quasicrystalline surface [J]. Journal of Alloys and Compounds, 2017, 712: 134−138.

[30] MISHRA S S, PANDEY S K, YADAV T P, SRIVASTAVA O N. Influence of chemical leaching on Al−Cu−Co decagonal quasicrystals [J]. Materials Chemistry and Physics, 2017, 200: 23−32.

[31] PANDEY S K, BHATNAGAR A, MISHRA S S, YADAV T P, SHAZ M A, SRIVASTAVA O N. Curious catalytic characteristics of Al−Cu−Fe quasicrystal for de/rehydrogenation of MgH_2 [J]. Journal of Physical Chemistry C, 2017, 121: 24936−24944.

[32] FORTY A J, DURKIN P. A micromorphological study of the dissolution of silver−gold alloys in nitric acid [J]. Philosophical Magazine A, 1980, 42: 295−318.

[33] JIN H J, KURMANAEVA L, SCHMAUCH J, RÖSNER H, IVANISENKO Y, WEISSMÜLLER J. Deforming nanoporous metal: Role of lattice coherency [J]. Acta Materialia, 2009, 57: 2665−2672.

[34] GRATIAS D, PUYRAIMOND F, QUIQUANDON M, KATZ A. Atomic clusters in icosahedral F-type quasicrystals [J]. Physical Review B, 2001, 63: 555−559.

[35] DUNEAU M. Covering clusters in the Katz−Gratias model of icosahedral quasicrystals [J]. Materials Science and Engineering A, 2000, 294: 192−198.

[36] UNAL B, JENKS C J, THIEL P A. Comparison between experimental surface data and bulk structure models for quasicrystalline AlPdMn: Average atomic densities and chemical compositions [J]. Physical Review B, 2008, 77: 195419.

[37] MCGRATH R, SMERDON J A, SHARMA H R, THEIS W, LEDIEU J. The surface science of quasicrystals [J]. Journal of Physics: Condensed Matter, 2010, 22: 084022.

[38] WANG Xiao-guang, WANG Wei-min, QI Zhen, ZHAO Chang-chun, JI Hong, ZHANG Zhong-hua. Novel Raney-like nanoporous Pd catalyst with superior electrocatalytic activity towards ethanol electro-oxidation [J]. International Journal of Hydrogen Energy, 2012, 37: 2579−2587.

[39] LIANG Z X, ZHAO T S, XU J B, ZHU L D. Mechanism study of the ethanol oxidation reaction on palladium in alkaline media [J]. Electrochimica Acta, 2009, 54: 2203−2208.

[40] YE Jian-qing, LIU Jian-ping, XU Chang-wei, JIANG San-ping, TONG Ye-xiang. Electrooxidation of 2-propanol on Pt, Pd and Au in alkaline medium [J]. Electrochemistry Communications, 2007, 9: 2760−2763.

快淬 $Al_{70}Pd_{17}Fe_{13}$ 准晶脱合金化制备纳米多孔钯及其电催化活性

刘歆翌，王英敏，羌建兵，王宝林，马殿国，张 伟，董 闯

大连理工大学 三束材料改性教育部重点实验室，大连 116024

摘 要：研究快淬 $Al_{70}Pd_{17}Fe_{13}$ 准晶在稀 NaCl 溶液中通过电化学脱合金化制备钠米多孔钯的过程，采用循环伏安法探讨纳米多孔钯在 1 mol/L KOH 溶液中对甲醇的电催化活性。XRD 和 TEM 分析表明，准晶晶粒在脱合金化初期发生纳米分解，当脱合金化完成后转变成纳米 FCC-Pd。SEM 观察表明，脱合金化样品中形成迷宫状的纳米多孔结构，孔径为 5~20 nm，纳米钯孔壁的晶体学取向无序，尺寸均匀，厚度约为 5 nm。EDS 测试结果表明，纳米钯孔壁中残留约 12 at.% Al。该纳米多孔钯在碱性环境中对甲醇显示明显的电催化活性。

关键词：纳米多孔钯；Al−Pd−Fe 准晶；脱合金化；电催化活性

(Edited by Wei-ping CHEN)